Galactic cosmic-ray ^{2}H/^{4}He and ^{3}He/^{4}He ratios revisited

B. COSTE[1], L. DEROME[1], D. MAURIN[1], A. PUTZE[2]
[1] *Laboratoire de Physique Subatomique et de Cosmologie, Université Joseph Fourier Grenoble 1, CNRS/IN2P3, Institut Polytechnique de Grenoble, 53 avenue des Martyrs, Grenoble, 38026, France*
[2] *The Oskar Klein Centre for Cosmoparticle Physics, Department of Physics, Stockholm University, AlbaNova, SE-10691 Stockholm, Sweden*
coste@lpsc.in2p3.fr

DOI: 10.7529/ICRC2011/V06/0175

Abstract: The B/C ratio is widely used in the literature to constrain cosmic-ray propagation parameters. In this work, we revisit the constraints set by the less-well studied quartet nuclei (^{1}H, ^{2}H, ^{3}He, and ^{4}He), and compare them to those set by other secondary-to-primary ratios (e.g., B/C). We compile destruction and production cross-sections as well as cosmic-ray measurements of light elements (^{2}H, ^{3}He, ^{2}H/^{4}He, and ^{3}He/^{4}He). This allows us to test the universality of propagation processes with species having different mass-to-charge ratios (A/Z). The parameters are derived using the USINE propagation package with a Markov Chain Monte Carlo (MCMC) technique. The latter is used to derive best-fit parameters, but also to obtain the 68% and 95% credible regions and correlations between the parameters. This proceeding presents some preliminary results; the full analysis will be given in Coste et al. (in preparation).

Keywords: Cosmic-ray propagation, light nuclei, Markov Chain Monte Carlo

1 Introduction

During the journey of Galactic cosmic rays (GCRs), from the acceleration sites to the solar neighbourhood, secondary CR species are produced due to nuclear interactions of heavier primary species with the interstellar medium. Hence, they are tracers of the CR transport in the Galaxy. Secondary-to-primary ratios, such as ^{2}H/^{4}He, ^{3}He/^{4}He, B/C, sub-Fe/Fe, are therefore suitable quantities to constrain the transport parameters for species $Z \leq 30$.

Most secondary-to-primary ratios have $A/Z \sim 2$. In that respect, ^{2}H/^{4}He and ^{3}He/^{4}He are unique since they probe a different regime and allow to address the issue of the 'universality' of propagation histories. For instance, an analysis in the leaky-box model (LBM) framework [5] finds that ^{3}He/^{4}He data imply a similar propagation history for light and heavier species (which was disputed in early papers). From the modelling side, after the first thorough and pioneering studies performed in the 60's-70's, the interest in the quartet nuclei stalled, and almost no dedicated studies can be found in the 00's. This is certainly related to the very slow publication pace of new data in this period. However, the most recent published data have not been properly interpreted yet, e.g., ^{2}H/^{4}He data from IMAX92, and ^{3}He/^{4}He data from IMAX92, SMILI-II, AMS-01, BESS98, and CAPRICE98. Furthermore, the analyses have commonly been performed in the successful but simplistic LBM. In this paper, we revisit the constraints set by the quartet nuclei and their consistency with the results of heavier nuclei, using the same diffusion model and MCMC technique discussed in [1, 2, 3].

2 Cross-sections

All reaction cross sections are taken from the parametrisation given by [6], except the proton-on-hydrogen (pH) reaction cross sections. The latter is evaluated from $\sigma_{pp}^{\rm inel} = \sigma_{pp}^{\rm tot} - \sigma_{pp}^{\rm el}$, where the total and elastic cross sections are fitted to the data compiled in the PDG[1]. Additionally, we had to renormalise the formulae given in [6] by a factor 0.9 for ^{4}He+^{4}He reactions in order to match the low-energy data. Figure 1 gives an illustration of the parameterisation along with data for X+H reactions.

The total secondary flux of CR species, originating from the interaction with the interstellar medium (ISM), results from the convolution of the cross sections and the measured primary fluxes. In principle, all nuclei must be considered, but the ISM and GCRs are mostly composed of ^{1}H and ^{4}He, making the reactions involving these species dominant. For heavier species, their decreasing number is balanced by their higher cross section. Note that ^{3}H is also produced in these reactions, but it decays in ^{3}He with a life time (12.2 years) short with respect to the propagation time. All tritium production is thus assimilated to a ^{3}He production for propagation, but the cross sections for this

1. http://pdg.lbl.gov/

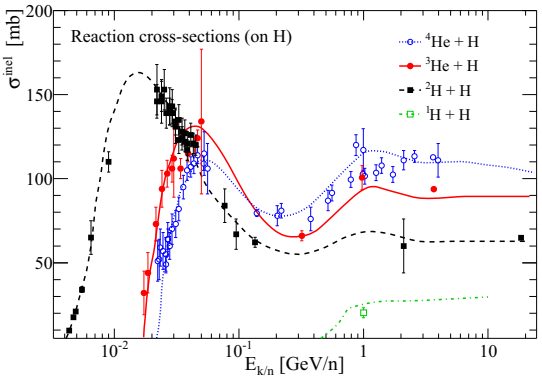

Figure 1: Total inelastic (reaction) cross sections for the quartet isotopes.

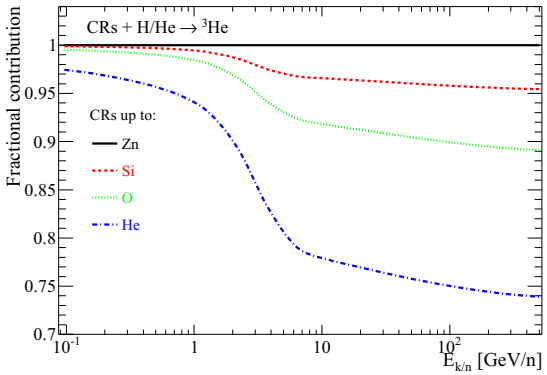

Figure 3: Fractional contribution from $A > 4$ CR nuclei to the ^{3}He flux as a function of energy.

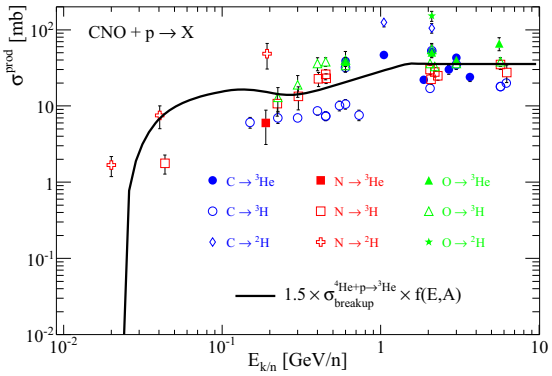

Figure 2: CNO + p → ^{2}H, ^{3}H, and ^{3}He cross sections.

fragment is provided as well. Depending on the precision sought for the calculation (as driven by the level of precision attained by current and forthcoming experiments), some of these contributions have to be taken into account. Moreover, we restrict ourselves to the straight-ahead approximation, which assumes that the kinetic energy per nucleon of the fragment is the same as for the projectile[2].

We compiled all accessible data for fragmentation of light nuclei on H and He, from projectile nuclei up to Zn. Figure 2 gives an illustration of the fragmentation of C, N, and O. The parameterisation relies mostly on the formulae given by [7], with several changes to better fit our extended set of data. For nuclear fragmentation cross sections of heavier nuclei, the concepts of 'strong' or 'weak' factorisation relies on the fact that at high energy, the branching of the various outgoing particles-production channels becomes independent of the target. This is discussed, e.g., in [9], where the authors conclude that though strong factorisation is probably violated, weak factorisation seems valid (see also, e.g., [10]). Consequently, this allows a scaling of cross-sections on a well known target such as ^{4}He to heavier targets. The full details and formulae will be given in Coste et al. (in preparation).

It is important to take the fragmentation from heavier nuclei into account. Indeed, at first order, the relative contribution to the ^{2}H and ^{3}He secondary production from $Z > 4$ nuclei with respect to the ^{4}He-induced production is proportional to their relative source term. For a secondary contribution, this source term is proportional to the primary flux of the parents (which have been measured by many experiments), and to the production cross-sections. This rough estimation is in agreement with the result of a full calculation in a realistic 1D diffusion model shown in Figure 3. Due to a preferential destruction of heavier nuclei at low energy, the primary-to-primary ratios are not constant. Indeed, heavier nuclei have larger destruction cross section, and therefore their propagated fluxes are more affected/decreased at low energy. This leads to a later reach of the plateau (of maximal contribution) at high energies. The observed trend is consistent with the primary-to-primary ratios shown in Fig. 14 of [3] for these ratios.

3 Data

Deuterons and ^{3}He fluxes are very sensitive to the modulation level, whereas ratios are less affected. In this analysis, we do not attempt to go beyond this force-field approximation, as speed is of essence for our MCMC analysis. We rely mostly on the force-field effective modulation parameter ϕ necessary to reproduce the data (as quoted in the seminal paper), but these values are slightly adjusted in order to give overlapping fluxes when all the data are demodulated

2. In practice, the energy of the fragments roughly follows a Gaussian distribution [7]. The impact on the secondary flux has been inspected for the B/C case by [8], where an effect $\lesssim 10\%$ was found. Given the large errors on the data used for this analysis, this effect can be ignored for the moment. However, future high-precision data (e.g. from the AMS-02 experiment) will probably need to take it into account.

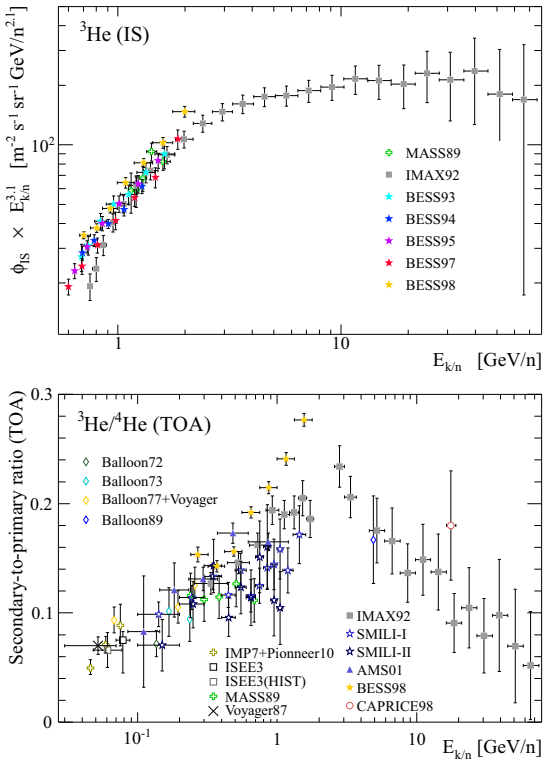

Figure 4: Top panel: demodulated interstellar (IS) ^{2}H fluxes times $E_{k/n}^{3.1}$. Bottom panel: top-of-atmosphere (TOA) secondary-to-primary ratio ^{3}He/^{4}He. References and the corresponding demodulation (for IS) and modulation (TOA) level ϕ are given in Coste et al. (in preparation).

and plotted together. Figure 4 shows a compilation of the ^{3}He flux (top panel) and the ^{3}He/^{4}He ratio.

4 Validation of the MCMC approach

MCMC techniques make the scan of high-dimensional parameter spaces possible. A direct consequence is the possibility of fitting simultaneously transport and source parameters [1]. However, on the one hand, transport parameters are strongly degenerate in the energy range 0.1-100 GeV/nuc [11]. On the other hand, source and transport parameters are correlated [1, 2]. In addition, primary fluxes (from which source parameters are mostly constrained) and secondary fluxes (from which transport parameters are mostly constrained) are not measured with the same accuracy, leading to a bias or even preventing an accurate determination of these parameters. This, although statistically correct, might not maximise the information obtained on the transport parameters. Therefore, we consider several strategies when dealing with these data.

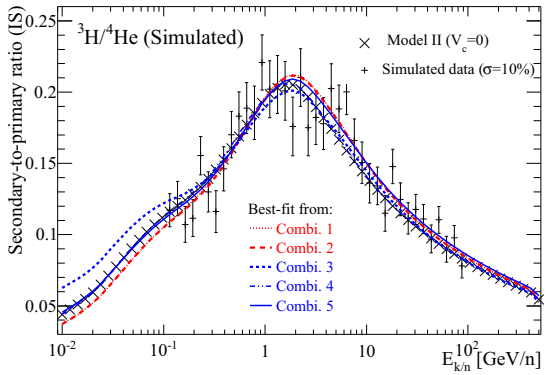

Figure 5: Analysis of the simulated data sets (plus symbols) for the ^{3}He/^{4}He ratio. The best-fit reconstructed curves correspond to the different combinations.

- a combined fit of secondary-to-primary ratios and primary fluxes in order to get the source and transport parameters simultaneously;
- a fit of the secondary-to-primary ratio only, either fixing the source parameters (i.e., using a strong prior), or using a loose prior.
- a fit of the primary flux only, either fixing the transport parameters (i.e., using a strong prior), or using a loose prior.

The different combinations are summarized in the following array.

Fitted parameters:	Data used for the fit:
1: transport + source	^{3}He/^{4}He + He ($\sigma_{\rm He} = 10\%$)
2: transport + source	^{3}He/^{4}He + He ($\sigma_{\rm He} = 1\%$)
3: transport + source	^{3}He/^{4}He
4: transport (source to 'true' value)	^{3}He/^{4}He
5: transport + source prior on source: $1.8 < \alpha < 2.5$ $-2 < \eta < 2$	^{3}He/^{4}He

As an illustration, the ^{3}He/^{4}He ratio and the corresponding simulated data (plus signs) are shown in Fig. 5. The statistical errors for the simulated data set correspond to the sigma of the standard Gaussian deviation used to randomise the data points around their model value. ^{3}He/^{4}He was generated with statistical errors of 10% while He fluxes were generated with 10% and 1% errors, to simulate a better measurement accuracy (in terms of statistics) than for secondary-to-primary ratios.

The various curves correspond to the sets of parameters given for each combination. As expected, the correct fit is recovered if the correct model is used and if there are no systematic uncertainties in the data. Actually, the MCMC allows us to retrieve more information from such an analysis. Indeed, one can access the full density probability

Table 1: Preliminary results: most likely and 68% CI on the transport parameters (^{3}He/^{4}He and PAMELA He flux [12]).

Data	δ	$K_0 \times 10^2$	V_a	V_c
-	-	(kpc^2 Myr^{-1})	(km s^{-1})	(km s^{-1})
^{3}He/^{4}He + He	$0.792^{+0.051}_{-0.041}$	$0.5^{+0.05}_{-0.06}$	$39.5^{+2.4}_{-2.6}$	$17.32^{+0.30}_{-0.44}$
^{3}He/^{4}He + ^{3}He + He	$0.79^{+0.03}_{-0.02}$	$0.76^{+0.08}_{-0.07}$	$48.1^{+1.9}_{-2.3}$	$19.59^{+0.27}_{-0.55}$
^{2}H/^{4}He + ^{2}H + He	$0.66^{+0.05}_{-0.06}$	$0.64^{+0.16}_{-0.09}$	$30.4^{+4.7}_{-3.5}$	$16.21^{+0.49}_{-0.57}$
B/C†	$0.86^{+0.04}_{-0.04}$	$0.46^{+0.08}_{-0.06}$	38^{+2}_{-2}	$18.9^{+0.3}_{-0.4}$

† Values taken from [2].

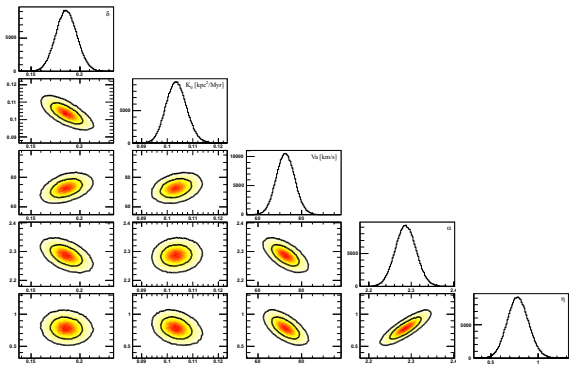

Figure 6: PDFs of parameters when constraining according to combination 1. Diagonals show marginalized PDF of each parameter while off-diagonal plots show joint PDFs.

functions (PDF) of the parameters. As an exemple, fig. 6 represents the marginalized and joint PDF of the parameters when applying the MCMC techniques to combination 1. In additions to most probable values of the parameters, errors and correlations are also clearly visible. This can be used to observe the degeneracy between transport and source parameters.

5 Preliminary results

Our preliminary results for the most-likely and 68% CI values on the slope δ and normalisation of the diffusion coefficient K_0, the value of the Alfvénic wind V_a, and the convective wind V_c are summarised in Table 1.

We note that adding the ^{3}He flux in the fit reduces the CI for some parameters, but increases it for others. As the quality of the ^{2}H/^{4}He data is poorer than for the ^{3}He/^{4}He, the CIs are larger (although several measurements of the ^{2}H flux help). Finally, we find that our best-fit model is the model with reacceleration and convection, which is also compatible with the result obtained from the B/C analysis of [13, 2]. We conclude that the quartet data is as powerful as B/C data to constrain the cosmic-ray transport parameters, and that forthcoming data from the PAMELA and the AMS-02 experiment should be helpful to further understand cosmic-ray propagation.

Acknowledgements

AP is grateful for financial support from the Swedish Research Council (VR) through the Oskar Klein Centre.

References

[1] Putze, A., Derome, L., Maurin, D., Perotto, L., & Taillet, R. 2009, A&A, 497, 991
[2] Putze, A., Derome, L., & Maurin, D. 2010, A&A, 516, A66
[3] Putze, A., Maurin, D., & Donato, F. 2011, A&A, 526, A101
[4] Ramaty, R. & Lingenfelter, R. E. 1969, ApJ , 155, 587
[5] Webber, W. R. 1997, Advances in Space Research, 19, 755
[6] Tripathi, R. K., Cucinotta, F. A., & Wilson, J. W. 1999, Universal Parameterization of Absorption Cross Sections - Light systems, Tech. rep., NASA Langley Research Center
[7] Cucinotta, F. A., Townsend, L. W., & Wilson, J. W. 1993, Nasa technical report, L-17139; NAS 1.60:3285; NASA-TP-3285
[8] Tsao, C. H., Silberberg, R., Barghouty, A. F., & Sihver, L. 1995, ApJ, 451, 275
[9] Olson, D. L., Berman, B. L., Greiner, D. E., et al. 1983, Phys. Rev. C, 28, 1602
[10] Michel, R., Gloris, M., Lange, H., et al. 1995, Nuclear Instruments and Methods in Physics Research B, 103, 183
[11] Maurin, D., Putze, A., & Derome, L. 2010, A&A, 516, A67
[12] Adriani, O. et al. 2011, Science, 332, 69
[13] Maurin, D., Donato, F., Taillet, R., & Salati, P. 2001, ApJ, 555, 585